

## Use of a Finite Element Code to Model Complex Mine Water Problems

Elfadil A. Azrag, Vladimir I. Ugorets, and Lee C. Atkinson

Hydrologic Consultants, Inc. of Colorado  
143 Union Boulevard, Suite 525  
Lakewood, Colorado, USA 80228  
email: hcico@hcico.com

### ABSTRACT

Numerical models are now used routinely to predict ground-water inflows to both surface and underground mines and to help design dewatering systems. Two of the more complex problems encountered in mine dewatering are 1) predicting the configuration of the phreatic surface and height of the seepage face in pit highwalls for slope stability analysis and 2) predicting inflow to underground mines, particularly from discrete geologic structures and under non-Darcian flow. Frustrated by the limitations of the most common ground-water flow codes in dealing with these problems, we have developed a 3-dimensional, finite element code, designated *MINEDW*, that has been specially designed to address the relatively unique hydrologic complexities of mining.

*MINEDW* includes subroutines to calculate the height of the seepage face in a pit wall, to simulate faults without adding more discretization, and to simulate non-Darcian flow and the transition to Darcian flow as heads and gradients decrease. Examples of *MINEDW* solutions to relatively idealized problems are given and compared to those from physical models, analytical solutions, and another numerical code (*MODFLOW*).

*MINEDW* has been applied to a large mining operation in Indonesia involving dewatering of both a large pit and underground drifts. This case has been made even more challenging by karstic features and very high, but variable (particularly as demonstrated by a recent El Niño-induced drought) precipitation. How the hydrogeology was conceptualized and incorporated into the numerical model, how the mine plans and variable precipitation were simulated, and the results of the calibration and predictive simulations are described.

### INTRODUCTION

In mining operations below the water table, two important water-related problems are potentially faced by mine operators. These are the amount and pressure of ground water that could flow into an underground excavation or an open pit and the effect of pore water pressure on the stability of an open pit highwall. For economic and safety purposes, it often is important to be able to predict the nature and magnitude of these potential problems so that appropriate dewatering or depressurizing systems can be installed.

Numerical models are now used routinely to predict ground-water inflows to both surface and underground mines and to help design dewatering systems. While adequate for addressing broad issues such as the impact of mining operations on regional water resources, many numerical

codes are limited in their ability to quantify the more detailed problems of the configuration of the phreatic surface in highwalls and inflows to underground openings. These limitations arise primarily from: 1) inadequate discretization, 2) poor representation of the height of seepage faces, and 3) disregarding the hydrodynamics of flow at and near discrete discharge points.

To overcome such limitations, *MINEDW*, a three-dimensional finite element ground-water flow code, was developed. The core of the code is based on algorithms previously developed by Durbin and Berenbrock (1985).

## DEVELOPMENT OF NUMERICAL FLOW CODE

*MINEDW* includes several subroutines to simulate the different aspects of ground-water flow in a mine setting. The governing equations underlying the algorithms in *MINEDW* are presented in the following sections.

### Governing Equations

The governing equation for three-dimensional, saturated-unsaturated flow of ground water under both Darcian and non-Darcian conditions is

$$\frac{\partial}{\partial x_i} (k_R K'_{ij} \frac{\partial h}{\partial x_j}) = S'_s \frac{\partial h}{\partial t} + W \quad (1)$$

where

- $h$  = hydraulic head [L],
- $k_R$  = relative hydraulic conductivity [ ],
- $K'_{ij}$  = effective hydraulic conductivity tensor [ $LT^{-1}$ ],
- $S'_s$  = effective specific storage [ $L^{-1}$ ],
- $t$  = time [T],
- $x_i$  = the Cartesian coordinate [L], and
- $W$  = all sources or sinks in terms of discharge per unit volume [ $T^{-1}$ ].

The effective hydraulic conductivity is derived from the classic Forchheimer equation for two-regime (i.e., both Darcian and non-Darcian) flow that, for an isotropic media, has the form

$$-\frac{dh}{dl} = \frac{1}{K} q + bq^2 \quad (2)$$

where

- $q$  = ground-water discharge in direction of flow [ $LT^{-1}$ ],
- $l$  = direction of ground-water flow [L],
- $K$  = hydraulic conductivity under Darcian flow conditions [ $LT^{-1}$ ], and
- $b$  = a coefficient [ $L^{-2}T^2$ ].

For the general case of saturated flow and where the media is anisotropic and  $l$  is arbitrarily oriented within a rectangular coordinate system, Equation 2 can be restated in the form

$$q_i = \sum_j \left( \frac{1}{\frac{1}{K_{ij}} + b_{ij}\bar{q}} \right) \frac{\partial h}{\partial x_j} \quad (3)$$

where

- $q_i$  = component of ground-water discharge in direction  $x_i$  [ $LT^{-1}$ ],
- $\bar{q}$  = resultant discharge within element [ $LT^{-1}$ ],
- $K_{ij}$  = hydraulic conductivity tensor for Darcian flow [ $LT^{-1}$ ], and
- $b_{ij}$  = tensor form of the coefficient  $b$  in Equation 2 [ $L^{-2}T^2$ ].

From Equation 3, the effective hydraulic conductivity tensor utilized in Equation 1 is described by

$$K'_{ij} = \frac{1}{\frac{1}{K_{ij}} + b_{ij}\bar{q}} \quad (4)$$

The location of the phreatic surface and the seepage face height (i.e., the height above the pit bottom of the point of intersection of the phreatic surface and the highwall) are calculated using an approximation to the saturated-unsaturated flow equations. This approximation utilizes a simple linear relationship between the hydraulic conductivity and the relative saturation of the prismatic element. To approximate the changes of the hydraulic conductivity associated with partially saturated conditions, the effective hydraulic conductivity is multiplied by a relative hydraulic conductivity factor (Equation 1). Below the phreatic surface, the relative hydraulic conductivity factor simply has a value of one. Above the phreatic surface, the hydraulic conductivity has a small value similar to the average rate of vertical percolation through the unsaturated zone. Thus, the relative hydraulic conductivity factor in an unsaturated element is set to a minimum value,  $k_{Rmin}$ . In a partially saturated element (i.e., one that contains the phreatic surface), the relative hydraulic conductivity factor is set equal to the ratio of the saturated thickness to the total height of the element. These conditions are expressed mathematically by

$$k_R(P) = \begin{cases} k_{Rmin} & \text{for } P_{bottom} < 0 \\ \frac{P_{bottom}}{H_E} & \text{for } P_{bottom} > 0 \text{ and } P_{top} < 0 \\ 1 & \text{for } P_{top} > 0 \end{cases} \quad (5)$$

where  $P$ , the pressure head [ $L$ ], is calculated from

$$P = h - x_3 \quad (6)$$

where the subscripts refer to the top or bottom of the prismatic element, and where

$H_E$  = height of element [L], and  
 $x_3$  = vertical coordinate [L].

As with most ground-water flow codes, the ground-water storage is comprised of two components, specific yield and specific storage. Below the phreatic surface, the specific storage,  $S_s$  [ $L^{-1}$ ], reflects the elasticity of the water and the compressibility of the media. Above the phreatic surface, *MINEDW* uses the following relationship to define the effective specific storage,  $S'_s$  [ $L^{-1}$ ]:

$$S'_s = k_R S_s \quad (7)$$

where  $K_R$  is the same as defined in Equation 5. At the phreatic surface, the specific yield (or drainable porosity) dominates the effective storage term due to the drainage of pore spaces. The governing equation is subject to the water-table boundary condition in the form:

$$K_i \frac{\partial h}{\partial x_i} n_i = -S_y \frac{\partial h}{\partial t} n_3 \quad (8)$$

and

$$h(x_1, x_2, z_w) = z_w(x_1, x_2) \quad (9)$$

where

$S_y$  = specific yield [ ],  
 $n_i$  =  $i$ th component of inward normal vector on water table [ ], and  
 $z_w$  = elevation of water table [L].

### Discharge of Ground Water

Drain nodes are used routinely to simulate discharge into an open pit, underground openings, or wells. In *MINEDW*, to further account for local resistance to flow at relatively constricted discharge points such as drifts or drainholes, the traditional drain node leakance factor is modified to:

$$C_L = \frac{K \cdot L \cdot w}{m \cdot \sqrt{\Delta h}} \quad (10)$$

where

$K$  = average hydraulic conductivity of material [ $LT^{-1}$ ],  
 $L$  = dimension of element [L],  
 $w$  = width of area [L],  
 $m$  = thickness of "skin" [L], and  
 $\Delta h$  = magnitude of change in head [ ].

The value for  $K$  is the computed average of the hydraulic conductivities (input values) of the elements around the drain node,  $L$  is a function of the grid discretization, and  $w/m$ , the so-called "connectivity factor", is a value obtained through calibration. Incorporation of the factor  $(\Delta h)^{1/2}$ , which is dynamically calculated by *MINEDW*, is deduced from the Darcy–Weisbach relationship for pipe flow. This factor simulates additional resistance to flow into a drift or drainhole immediately after their installation when the gradient into them is high (i.e.,  $\Delta h$  is large). However, when the gradient decreases, the  $(\Delta h)^{1/2}$  factor becomes smaller. Thus, the leakage factor becomes larger, resulting in less resistance to inflow.

### Other Special Features of *MINEDW*

*MINEDW* includes the conventional simulation packages such as evapotranspiration, ground water/surface water interaction at streams and springs, and stream routing. *MINEDW* also has a number of other special features, however, that were specifically designed to improve simulation of ground-water flow in the immediate vicinity of mines. These features include:

- Removal of elements and nodes to simulate excavation of a pit,
- Calculation of seepage faces in highwalls,
- Fault linking,
- Specified-flux or specified-head boundary conditions that, coupled with the fault-linking routine, can simulate pumping from multiple levels in a well,
- Variable-flux boundary conditions,
- Simulation of pit infilling, and
- Ability to use either a collapsing or rigid grid.

Each of these special features will be described briefly.

To simulate excavation of a pit, *MINEDW* removes elements and corresponding inactive nodes. The input file defines the elements representing the excavation that are to be removed at a specified time step. The input file also includes a table of node elevations vs. time according to the mine plan so that *MINEDW* can gradually decrease the nodal elevations per the mine plan until such time as the element is ultimately removed.

The potential occurrence of a seepage face in the highwalls of a pit is simulated using the remaining nodes (i.e., those that have not been removed) that define the surface of the excavation.

The input file specifies these as seepage face nodes with one of the two special properties: 1) a zero pressure if the calculated hydraulic gradient at them is outward (i.e., into the pit) or 2) a zero flow if the hydraulic gradient at them is inward (i.e., into the highwall). *MINEDW* automatically inserts additional elements and nodes on the surfaces of the excavation in each time step to increase grid discretization.

*MINEDW* can simulate the effect of highly conductive zones such as faults without requiring the addition of discrete elements to the model grid. The so-called "fault linking" is accomplished by specifying node pairs which are coupled with a large (user specified) transmissivity. The effect is to simulate enhanced movement of ground water between the linked nodes in addition to the normal calculation of flow between all nodes within the elements.

The fault-linking routine can also be used in conjunction with either a specified-flux or specified-head boundary condition to simulate pumping from a dewatering well whose production interval spans two or more nodes. The fault-linking routine, which causes the head to be essentially the same at all of the fault-linked nodes representing the well, results in the component of discharge from each interval being proportional to the transmissivity of the interval.

Similar to most ground-water flow codes, *MINEDW* can incorporate both specified-head and specified-flux boundary conditions. As an alternative to the third-type boundary conditions used in some codes (e.g., the General Head Boundary of *MODFLOW*) that require questionable assignment of reference heads and distances, *MINEDW* also can incorporate a variable-flux boundary condition. This technique attaches an analytical representation of an infinite, linear or radial aquifer to the boundary of the model grid. In effect, the variable-flux boundary condition extends the model area to infinity. It then calculates variable fluxes at the boundary as a function of the extrapolated changes in water levels beyond the model domain based on the transmissivity and storativity of the extended aquifer.

*MINEDW* can simulate passive infilling of a pit or underground mine after mining has been completed and dewatering has ceased. This simulation requires as input the relationship between the water level and the volume of water in the pit or mine at any time. If significant, evaporation from the surface of a "pit lake" can also be incorporated into the simulation. A more complete description of this feature of *MINEDW* is given by Naugle and Atkinson (1992). Another application of the pit lake infilling routine is to quantify the components of inflow from various lithochemical zones as input to hydrogeochemical modeling of ultimate pit lake water quality (Bird and Mahoney, 1994).

*MINEDW* can utilize either a deforming or a rigid grid. Selection of the method is usually based on the nature of the problem to be solved (e.g., when simulation of seepage faces is desired, the rigid grid must be used). When the deforming grid option is selected, the code solves the ground-water flow equation only in the saturated part of the model domain; and the grid deforms upward or downward to accommodate changes in the location of the phreatic surface. If the downward movement of the phreatic surface crosses a boundary between hydrogeologic units of different hydraulic properties, the code automatically adjusts the properties of the elements accordingly. If the rigid grid option is selected, *MINEDW* uses the saturated-unsaturated relationship described by Equation 1 to solve the problem.

### VERIFICATION PROBLEMS

Three problems will be described that verify some of the special features of *MINEDW*.

#### Variable Flux Boundary Condition

This first problem compares the results from the variable flux boundary condition that is implementable with *MINEDW* to those from an analytical solution for one-dimensional flow in a confined, homogeneous, isotropic aquifer of semi-infinite extent. Inserting hydraulic parameters into the solution for heat flow in a semi-infinite solid with a constant temperature at the finite boundary that was developed by Carslaw and Jaeger (1959):

$$h(x,t) = h_o \operatorname{erfc} \left( \frac{x}{2 \sqrt{\frac{Kt}{S_s}}} \right) \tag{11}$$

where

- $h(x,t)$  = hydraulic head at distance  $x$  and time  $t$  [L],
- $h_o = h(0,t)$ , constant hydraulic head at boundary  $x = 0$  [L],
- $x$  = distance from finite boundary [L], and
- $t$  = time [T].

To solve the problem numerically, a finite element grid was constructed with 180 nodes and 116 elements in a single layer 3 m thick. The rectangular grid has a length of 1,768 m and a width of 12.2 m. The strip aquifer is assigned a hydraulic conductivity of 30.5 m/day and a specific storage of  $3.28 \times 10^{-3} \text{ m}^{-1}$ . The initial head at all locations is 0.0 m, and the constant head applied at the  $x=0$  boundary beginning at  $t=0$  is 3 m. The initial time step is 0.25 day, and subsequent time steps are increased by a factor of 1.3.

Figure 1 shows the heads at various times at a distance of 304.8 m from the constant head boundary obtained from *MINEDW* and from Equation 11.

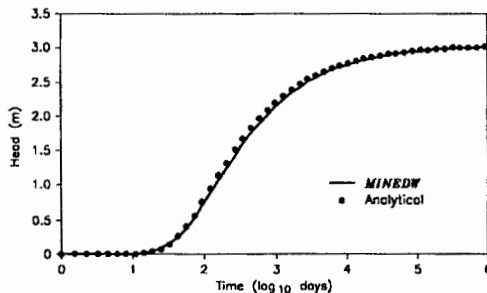


Figure 1: Comparison of results from *MINEDW* and analytical solution.

### Development of Seepage Face

In this second problem, results from *MINEDW* are compared to those from a laboratory investigation of development of a seepage face in a porous media (Hall, 1955). From the series of tests performed with a physical model (summarized in Table 1 of Hall, 1955), Test No. 6 (Series A) was selected for validation of *MINEDW*. In that test, a constant head of 1.22 m was maintained at the outer boundary of the 15-degree, pie-shaped model at a radial distance of 1.95 m while the head in the well was adjusted to 0.30 m. The sand used in the model had a hydraulic conductivity of about 400 m/day. Under these conditions, the flow rate was 0.345 L/sec, and the height of the seepage face was 0.54 m above the water level in the well (Hall, 1955).

A 15-degree, pie-shaped finite element grid consisting of 561 nodes, 640 elements, and 10 layers each 0.15 m thick was developed to replicate the Hall model. The radial grid spacing originates at 0.12 m (the radius of Hall's "well") and increases logarithmically to the outer radial boundary at a distance of 1.95 m.

The comparison of the heads calculated by *MINEDW* and those measured in the laboratory by Hall (1955) are shown in Figure 2. Using a  $K_{Rmin}$  value of 0.001, *MINEDW* calculated a seepage face height of 0.49 m and a discharge rate of 0.340 L/sec, within about 10 and 1.5 percent, respectively, of the results obtained by Hall (1955).

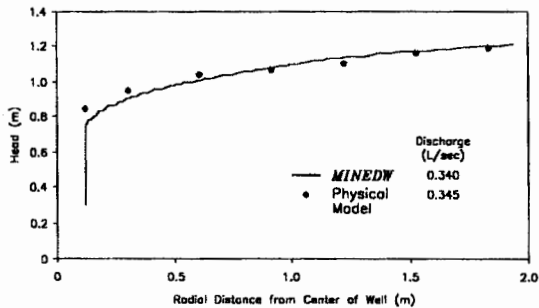


Figure 2: Comparison of results of *MINEDW* and Hall (1955) physical model.

### Steady-State, Unconfined, Non-Darcian, Radial Flow to Circular Pit

The objective of this third problem was to further validate the saturated/unsaturated flow, non-Darcian flow, and seepage-face routines incorporated into *MINEDW*. The results of numerical models utilizing both *MINEDW* and *MODFLOW* are compared to the results of a physical model tested by Dudgeon (1985).

Dudgeon (1985) constructed a 90-degree, circular, unconfined "aquifer" with a thickness of about 1.1 m and an outer boundary at a radial distance of 2.4 m. His partially penetrating "circular pit" had a radius of 0.59 m. The granular material comprising the aquifer had a hydraulic conductivity of 0.06 m/s, and the value of  $b$  (Equation 2) derived from two-regime permeameter tests was 2,100  $s^2/m^2$ .

The finite element grid used to replicate the physical model consisted of a logarithmically discretized radial grid and 16 layers representing a total aquifer thickness of 1.2 m. There is a total of 2,312 nodes. The partially penetrating pit was simulated by removing the uppermost 12 layers of elements within the ring of nodes corresponding to the radius of the pit. Constant heads of 0.835 m and 1.09 m were assigned at the floor of the pit and at the model boundary, respectively, simulating the conditions utilized by Dudgeon (1985) in his physical experiments.

For the simulation using *MINEDW*, the  $K$  and  $b$  values derived by Dudgeon (1985) were directly input to the non-Darcian flow routine of the code. The *MINEDW*-based model was then run under steady-state conditions. The calculated seepage face height of 0.065 m compared favorably with the measured height of 0.045 m (Dudgeon, 1985). The calculated and measured inflows were both 25.4 L/sec.

For the simulation using *MODFLOW*, a finite difference grid consisting of 42 rows and 42 columns of cells equally spaced at 0.059 m and 16 layers (for a total of 28,224 cells) was developed. Cells inside the circular pit boundary were designated inactive. The seepage face was simulated using the *MODFLOW* drain package with the drain height specified as the height of the centers of the drain cells, corresponding to a  $P=0$  condition. The same constant head of 0.835 m and 1.09 m were assigned at the floor of the pit and at the model boundary, respectively.

The *MODFLOW*-based model was also run under steady-state conditions. The inflow to the pit predicted by *MODFLOW* was 41.6 L/sec, about 60 percent greater than the experimentally observed inflow. The solution did not predict development of a seepage face.

The results of the laboratory investigation and the two numerical simulations are summarized in Figure 3.

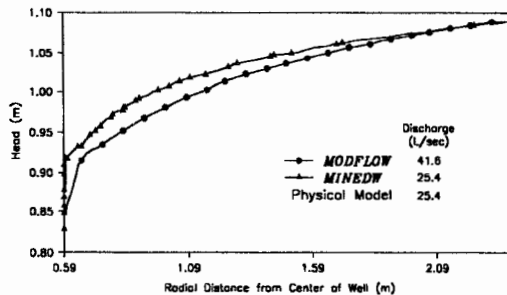


Figure 3: Comparison of results of numerical models and Dudgeon (1985) physical model.

## APPLICATION TO A COMPLEX MINE WATER PROBLEM

*MINEDW* has been used to develop a multi-purpose ground-water flow model of a large, combined open pit and underground mining operation in Indonesia. One of the objectives of the model was to predict ground-water inflows to various underground workings that would comprise the primary source of water for the mill during periods of El Niño-induced drought.

The area modeled encompasses more than 100 km<sup>2</sup> and includes predominantly carbonate rocks about 2,000 m thick with a series of dioritic intrusions. The model grid contains 13,182

nodes and 22,722 elements which have been discretized to represent the most important hydrogeologic features. Regionally, the model has six layers; but in the pit area there are nine layers to represent both the geology and mining in greater detail. Eighteen different hydrogeologic units were incorporated into the model, and thirteen major faults and highly permeable contact zones around the various intrusives bodies have been simulated using the fault-linking routine of *MINEDW*. A total of 77 springs and 30 streams have been incorporated into the model using drain and river nodes.

Both historic and future surface and underground mining were incorporated into the model using the special subroutines in *MINEDW*. The various drifts, drainholes, and block cave areas are represented by 511 drain nodes that are "turned on" at times according to actual historic mining or as specified by the mine plan. For the transient calibration, historic precipitation, which has been variable both in time and space, was applied to the 1,668 surface nodes of the model using 30-day time steps. The parameters to which the model were calibrated included the hydraulic properties (hydraulic conductivity, specific storage, specific yield) of the various hydrogeologic units, the transmissivity and non-Darcian flow characteristics (i.e., the value for  $b$  in Equation 2) of the fault zones, and the connectivity factor for the drain nodes (Equation 10). The calibration was most sensitive to the transmissivity of the faults and the connectivity factors of drain nodes. These parameters were varied during the calibration process until an acceptable match had been obtained between calculated and measured inflows to the two main drifts and their associated drainholes (Figure 4).

After the model had been calibrated, predictive simulations were made by incorporating the current mine plan and stochastically generated predictions of future, variable precipitation (including simulation of an El Niño-induced drought period). Figure 4 shows the predicted inflows. The oscillations in the predicted inflows are a result of extreme variations in precipitation. The general decrease in inflows to Drift A beginning about year 2004 is associated with the completion of the majority of the primary underground excavations, depletion of storage in the ground-water system, and reaching of quasi-steady state conditions subject only to variations in precipitation.

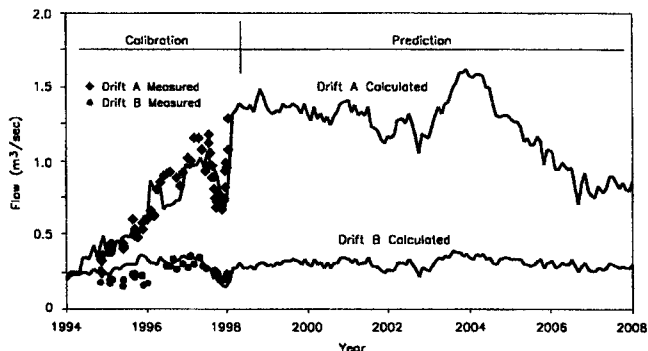


Figure 4: Calibration results and predictions of inflows to drifts.

## CONCLUSIONS

Numerical ground-water flow models which have the ability to simulate seepage faces in highwalls and non-Darcian flow to surface and underground mines result in a more reasonable understanding of the detailed nature of flow in the immediate vicinity of mines. Numerical experimentation with and actual application of *MINEDW* to field problems indicate that such enhanced modeling produces significant information that can have both favorable and unfavorable ramifications. The good news is that non-Darcian flow can have a significant effect in throttling back the inflow to a mine that would otherwise occur under totally Darcian flow. However, this same resistance can result in higher seepage faces and phreatic surfaces in pit highwalls. In any case, such knowledge can be important input to planning dewatering and in slope stability analysis.

## REFERENCES

- Bird, D.A. and J.J. Mahoney, 1994. Estimating Post-Mining Pit Lake Geochemistry Utilizing Geochemical and Numerical Modeling. Reprint No. 94-241 of paper presented at 1994 Annual Meeting of Society for Mining, Metallurgy, and Exploration, Albuquerque, New Mexico, 5 pp.
- Carslaw, H.S. and J.C. Jaeger, 1959. Conduction of Heat in Solids. Oxford University Press, London, 510 pp.
- Dudgeon, C.R., 1985. Effects of Non-Darcy Flow and Partial Penetration on Water Levels Near Open Pit Excavations. In Hydrogeology in the Service of Man, Memoirs of 18th Congress of International Association of Hydrogeologists, Cambridge, pp. 122-132.
- Durbin, T.J. and C. Berenbrock, 1985. Three-Dimensional Simulation of Free-Surface Aquifers by the Finite Element Method. U.S. Geological Survey Water-Supply Paper 2270, pp. 51-67.
- Hall, H.P., 1955. An Investigation of Steady Flow Toward a Gravity Well. La Houille Blanche, v. 10, pp. 8-35.
- Naugle, G.D. and L.C. Atkinson, 1993. Estimating the Rate of Post-Mining Filling of Pit Lakes. Mining Engineering, v. 45, no. 4, pp. 402-404.